

Available online at [www.sciencedirect.com](http://www.sciencedirect.com)

ScienceDirect

Procedia CIRP 55 (2016) 182 – 187

[www.elsevier.com/locate/procedia](http://www.elsevier.com/locate/procedia)

5th CIRP Global Web Conference Research and Innovation for Future Production

## Tools and strategies for grinding of riblets on freeformed compressor blades

B. Denkena, T. Grove, T. Krawczyk\*

*Leibniz Universität Hannover, Institute of Production Engineering and Machine Tools, An der Universität 2, 30823 Garbsen, Germany*\* Corresponding author. Tel.: +49-511-762-19937; fax: +49-511-762-5115. E-mail address: [krawczyk@ifw.uni-hannover.de](mailto:krawczyk@ifw.uni-hannover.de)

### Abstract

A major goal in the design of turbomachinery is the increase of efficiency. To attain this increase, the flow losses must be reduced. A substantial proportion of the losses is generated by skin friction between compressor blades and working fluid. With respect to smooth surfaces, micropatterns (riblet-structures) reduce skin friction in turbulent flow by up to 10 %. Grinding with multiprofiled wheels is an effective method for the manufacturing of riblet-structures on large plane surfaces. However, the grinding wheel wear affects the accuracy of the riblet geometry and the efficiency of the manufacturing process. Therefore, this paper shows the potential of different grinding wheel types for the manufacturing of riblet structures on an industrial scale with regard to tool wear. The results show that vitrified bonded tools are not suitable for the structuring of compressor blades. Here, axial forces lead to high profile wear. In contrast, grinding wheels with a metal bond are more wear resistant. However, the dressing process of metal bonded tools is time-consuming and causes 80% of the total machining time. As a consequence, just one blade can be structured per day. To increase the efficiency, a new grinding wheel was developed, which is bionically inspired by beaver teeth. The tool is constructed of alternating layers consisting of metal bonded diamonds and pure resin respectively. With this layer-by-layer setup, the tool does not have to be dressed and enables structuring of up to 50 compressor blades per day.

© 2016 The Authors. Published by Elsevier B.V. This is an open access article under the CC BY-NC-ND license (<http://creativecommons.org/licenses/by-nc-nd/4.0/>).

Peer-review under responsibility of the scientific committee of the 5th CIRP Global Web Conference Research and Innovation for Future Production

*Keywords:* grinding, micro pattern, grinding wheel design, riblets

### 1. Introduction

Bionic structures have exceptional properties. For example, lotus leaves are dirt-repellent due to micro patterns on their surface (lotus effect) [1]. Geckos have branched nanohairs on the feet to cling on virtually any surface (gecko effect) [1]. Another important micro pattern, which can be used in the industry, can be found on shark skin. The skin of a shark is not smooth. Due to small ribs, called riblets, the skin feels rough. Investigations show that ideal riblets reduce skin friction up to 10 % [1,2]. Skin friction limits the efficiency of different continuous-flow machines like pumps or turbines [3]. Therefore, the use of riblets structures in the industry has great potential (fig. 1). For example, ideal riblets with an aspect ratio of 0.5 and a width between 20  $\mu\text{m}$  and 60  $\mu\text{m}$  can improve the efficiency of a turbine by about 0.2% [4]. As a result, about 400,000 t kerosene can be saved per year. The benefit of riblets in pumps is even higher. Here, riblets increase the efficiency

about 1.5 %. Pumps are the largest energy consumers in industry [5].

#### Nomenclature

$a_c$	depth of cut
$b_s$	width of the grinding profile
CBN	cubic boron nitride
$F_a$	axial force
$h$	riblet-height
$l_{\max}$	maximum contact length
$r_{\text{eq,max}}$	maximum equivalent grinding wheel radius
$R_{\max}$	maximum grinding wheel radius
$R_{\text{path}}$	tool path radius
$R_{\text{WZ}}$	workpiece radius
$R_{\text{WS}}$	grinding wheel radius
$s$	riblet-width
SIC	silicon carbide

$v_c$	cutting speed
$v_f$	feedrate
X	axis
$X_L$	length in X direction
Z	axis
$Z_B$	width in Z direction
$\alpha$	angle
$\Delta r_{sw}$	radial profile wear
$\Delta r_0$	radial profile wear after 0 mm grinding length
$\Delta r_{1300}$	radial profile wear after 1300 mm grinding length
$\sigma_{max}$	maximum stresses

To use the potential of micro patterns, manufacturing processes are required, which economically generate micro patterns in a high quality. Compared to laser machining, EDM, micro milling and micro planing, grinding with multi-profiled wheels has been established as an effective method for generating riblet-structures on large scale surfaces [6]. So far, riblet-structures with an aspect ratio of 0.5 and a width of 60  $\mu\text{m}$  have been ground on single curved NACA6510 profiles whereby a reduction of the near wall friction of about 4 % has been achieved [7]. In contrast to NACA-profiles actual compressor blades have double curved or freeform surfaces. These surfaces have to be machined employing a five-axis-grinding process. Therefore, additional requirements on the grinding process (such as complex contact conditions) have to be considered [8]. For example, the tool paths have to be curved in order to follow the curved stream flow. Such complex tool paths were used for example for belt-grinding in mould manufacturing [9].

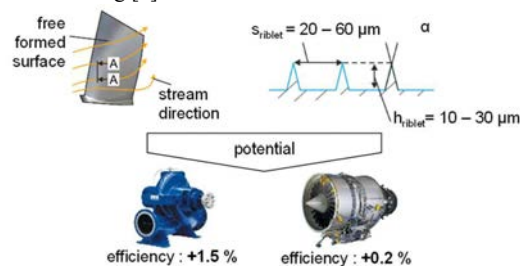


Fig. 1. Benefits of riblet-structures

The effect of five-axis motion on the ground riblet-structures is unknown. To close the research gap in structuring of freeform surfaces, the relevant influencing factors on the accuracy of the riblet-geometry in five-axis-grinding of riblet structures on double curved compressor blades are investigated. Thus, this paper considers the potential of different grinding wheel specifications for the manufacturing of riblet structures on an industrial scale with regard to tool wear.

2. Grinding wheel geometry

Grinding of riblets on flat surfaces with a straight tool path is well investigated [6]. In this process the ground groove is influenced only by the shape of the grinding wheel profile. Due to the straight contact length, the process kinematic can affect the riblet-geometry in case of five-axis-grinding. To investigate the influence of the five-axis-kinematic on the riblet quality,

grinding experiments were done. The workpieces were made of soft obomodulan material in order to neglect tool wear.

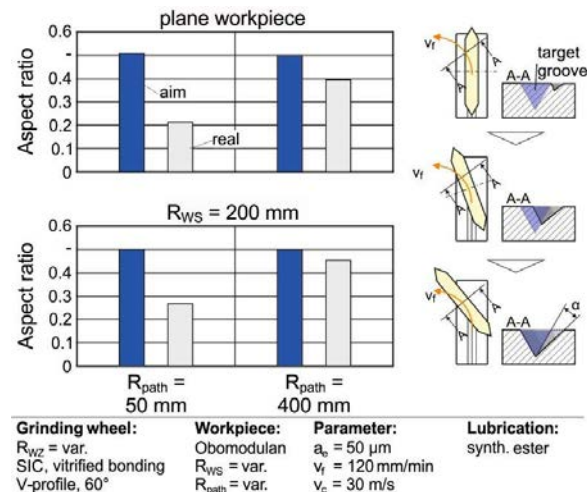


Fig. 2. Expected and real aspect ratio for five-axis grinding

Fig. 2 illustrates the effect of tool path and workpiece radius on the aspect ratio. Riblets with an aspect ratio of nearly 0.5 were only obtained for  $R_{path} \geq 400 \text{ mm}$  and a curved workpiece. In all other cases, smaller aspect ratios were obtained. Smaller tool path radii and larger convex workpiece radii lead to a decreased aspect ratio. As a result, flat workpieces and a tool path radius of 50 mm generates the smallest aspect ratio of 0.2. This deviation from the ideal case is caused by undercuts resulting from the contact conditions of grinding wheel and workpiece. On the right of Fig. 2, it is illustrated how undercuts occur. To grind ideal riblets, the target groove has to be ground in cross section A-A. Due to the straight contact length, the grinding wheel removes in cross section A-A material outside of the target groove. When the grinding wheel moves forward on the curved tool path, the remaining material will be removed and an undercut results. As a consequence, the width of the ground groove will be enlarged and the face angle of the groove differs from the targeted one. Undercuts can be avoided when the contact length is small enough and the contact area fits into the target groove. Since the tool path radius is defined by the streamflow and therefore fixed, the grinding wheel geometry must be adapted to prevent the occurrence of undercuts.

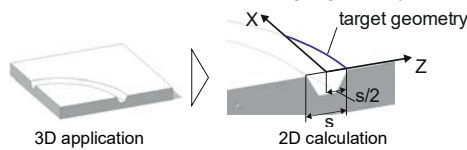
This knowledge was used to calculate the maximum applicable diameter of the grinding wheel in dependence on the tool path radius. The mathematical description of the target geometry that is needed for the calculation of the maximum grinding wheel diameter bases on a 2D calculation (fig. 3). Here, the target geometry is represented by a circle segment within a coordinate system. The coordinate origin is located in the centre of the groove. The circle segment starts at  $(0, Z=s/2)$ .

The maximum contact length is calculated in the next step. In order to grind ideal riblets, the whole contact length must fit into the target geometry. Otherwise, undercuts occur. The position of maximum contact length depends on Z. In case of a triangular grinding wheel profiles, the maximum contact length is in the centre of the groove. For grinding wheels with

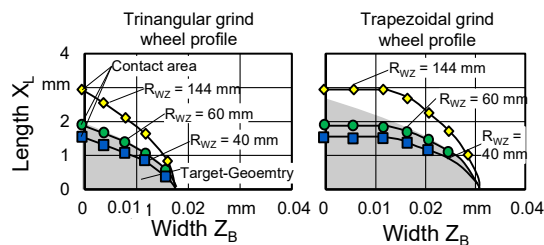
trapezoid shaped profiles the maximum contact length is at a different Z-position.

The position of the maximum contact length and the formula for the target geometry are used to calculate the maximum contact length. For flat workpieces the maximum grinding wheel diameter is a function of contact length and the depth of cut. To get the maximum grinding wheel radius for curved workpieces one additional step is necessary. Here, the contact length and depth of cut are used to calculate the equivalent grinding wheel radius. Normally, the equivalent grinding wheel radius will be calculated to compare flat and cylindrical grinding. The equivalent grinding wheel radius is a function of depth of cut, workpiece curvature and actual workpiece radius. With transforming the formula the grinding wheel radius can be calculated.

### 1. Mathematical description of the target geometry



### 2. Calculation of the maximum contact length ( $l_{max}$ )



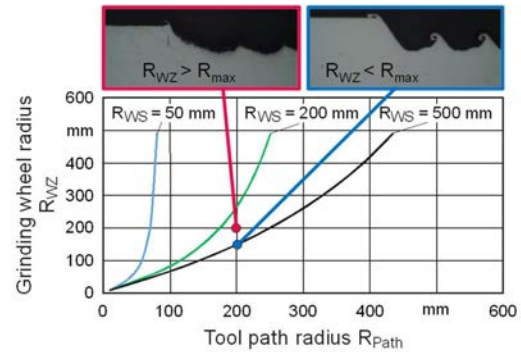
### 3. Calculation of the maximum grinding wheel radius

$$r_{eq,max} = \frac{l_{max}^2 + a_e^2}{2 \cdot a_e} \quad R_{WZ} = \frac{R_{WS} \cdot r_{eq,max}}{R_{WS} - r_{eq,max}}$$

Fig. 3. Calculation of grinding wheel geometry

Fig. 4 shows the maximum radius of the grinding wheel as a function of tool path radius for different workpiece radii. The calculations were done for a depth of cut of 0.05 mm. The maximum grinding wheel radius increases with larger tool path radii. This behavior is independent of the workpiece radius. In case of equal tool path radii, smaller workpiece radii allow larger grinding wheel diameters. This relation can be explained with the contact length. For a constant grinding wheel diameter and depth of cut, the contact length depends on the workpiece radius. Compared to grinding of plane surfaces, the contact length increases for larger concave curvatures. A larger convex curvature of the workpiece decreases the contact length. The calculation method assumed that each tool path radius has one maximum contact length in order to grind ideal riblets (fig. 3). If the contact length is decreased by the workpiece curvature, the grinding wheel radius can be increased to obtain the same maximum contact length. In addition to these calculations, grinding experiments were done. For these experiments the maximum grinding wheel radius was defined for a tool path radius of 200 mm, workpiece radius of 500 mm and a depth of cut of 0.05 mm. To verify the model, different grinding wheels

were used. The first grinding wheel has a radius of 150 mm and should therefore be able to grind ideal structures. The other grinding wheel had a radius of 200 mm. This radius is larger than the calculated maximum grinding wheel radius and undercuts should occur. The results of the grinding experiments are shown in Fig. 4, top. The first tool generates ideal riblets (blue frame) at a tool path radius of 200 mm. In contrast to that, the use of the grinding wheel with a radius of 200 mm leads to undercuts and defects on the riblets (red frame). These results are in agreement with the maximum contact area model.



Grinding wheel:	Workpiece:	Parameter:	Lubrication:
$R_{WZ} = \text{var.}$	X20Cr13	$a_e = 50 \mu\text{m}$	synth. ester
SIC, vitrified bonding	$R_{WS} = \text{var.}$	$v_f = 120 \text{ mm/min}$	
V-profile, 60	$R_{\text{path}} = \text{var.}$	$v_c = 30 \text{ m/s}$	

Fig. 4. Verified model to define a grinding wheel geometry

## 3. Grinding wheel specification

The calculation of the grinding wheel geometry is the first step in the process design. In order to grind riblets on a freeform surface the right process parameter and grinding wheel specifications are necessary. Therefore, the influence of feedrate, spindle speed, depth of cut and grinding wheel specification on tool wear are investigated.

### 3.1. Vitrified bond

Wang has shown that grinding wheels with a vitrified bond and SIC grains are suitable to grind riblets with a width of 60  $\mu\text{m}$  on a length of 1000 mm [6]. Longer grinding lengths and smaller riblet-dimensions require grinding wheels with a CBN grain and bonds with a better wear behavior [6].

To transfer the results on freeform surfaces, vitrified bonded SIC grinding wheels were used for the structuring of curved surfaces. The maximum tool radius was calculated for a minimal tool path radius of 200 mm. The process parameters values were equal to those used by Wang [6]. After dressing, the grinding wheel profile had a height of 40  $\mu\text{m}$  at a width of 60  $\mu\text{m}$ . The expected grinding wheel wear was 10  $\mu\text{m}$ . These parameters and the grinding wheel geometry should lead to riblets with a width of 60  $\mu\text{m}$  and an aspect ratio of 0.5. In all experiments smaller aspect ratios result (fig 5, top). Smaller workpiece radii lead to an increase in the difference between the expected and real aspect ratio. However, the grinding wheel geometry is suitable for grinding ideal riblets on freeform surfaces. For this reason, the deviation is solely caused by higher profile wear. To investigate the wear behavior in detail

and explain the unexpected aspect ratio, additional grinding experiments were conducted in which the workpiece radius and the tool path radius were changed. Each experiment was repeated four times. The wear behavior was analyzed after the first cut and after a grinding length of 1300 mm. Fig. 5, bottom, summarizes the results. Independent of the workpiece radius, the smaller tool path radius leads to higher profile wear in the first cut. This relation is stronger for an increased workpiece curvature. However, the initial profile wear affects the following wear behavior. Low profile wear in the first cut results in higher wear on the following grinding length. As a result, the radial profile wear after a grinding length of 1300 mm depends just on the workpiece radius. It can be assumed that the initial profile wear leads to a grinding profile geometry which is more wear-resistant. This high influence of the workpiece radius can be explained by the material removal behavior. A grinding wheel, which moves on a curved surface, removes more material after the same length than on a flat surface. The material removal does not explain the impact of the tool path radius on the tool wear because the chosen grinding wheel diameter was suitable to grind without undercuts.

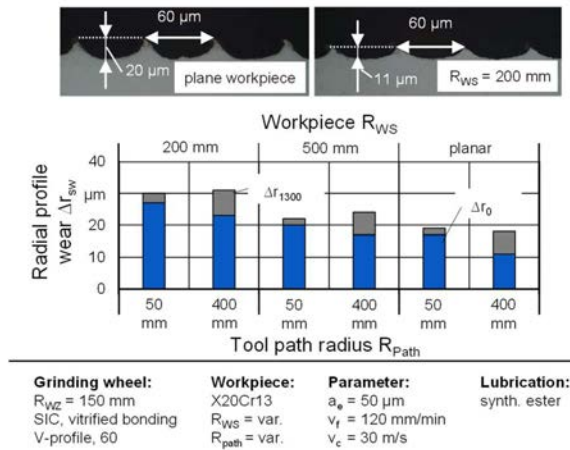


Fig. 5. Profile wear as a function for workpiece and tool path radius

To explain the initial tool wear, process forces were investigated (fig. 6). In contrast to grinding of straight riblets, curved tool path radii cause axial forces. In case of a straight tool path, both sides of the grinding wheel profile remove the same material volume. As a consequence, the axial forces cancel each other out. When grinding with a curved tool path, both sides of a profile remove a different volume of material: the inner profile side removes more material than the outer side. Consequently, the axial forces do not cancel each other out. The difference in the removed material volume between both sides increases with smaller tool path radii. That is why a smaller tool path radii lead to an increased axial force. However, it's not clear if the axial force is high enough to produce profile wear.

To investigate the influence of the axial force on the tool wear, an FEM simulation model was established with Ansys. The model is used to answer the question whether it is possible, that the axial forces cause stresses which are high enough to result in tool wear. The simulation consists of a grinding wheel

model and an axial load. The grinding wheel profile is represented by a homogeneous structure and its geometry is identical to the real profile, which exists after the dressing process. This profile was loaded with the axial forces and the stress distribution was analyzed. Maximum stresses of 28 MPa are situated at the tip of the grinding wheel profile. Linke showed in her investigations that grinding wheel profiles with different specification break when stresses between 23 and 36 MPa occur [10].

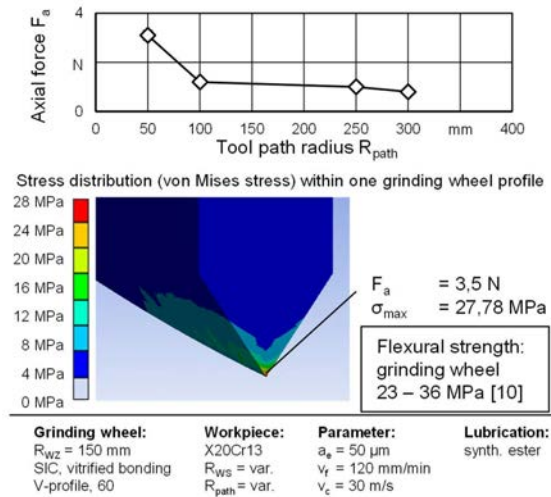


Fig. 6. Axial force and stress distribution

This means that the axial forces cause stresses which are high enough for profile breaks to occur and the profile wear behavior can be explained.

### 3.2. Metal bond

In contrast to vitrified bonded tools, grinding wheels with a metal bond and CBN-grains show a better wear behavior. Wang has shown that these tools are suited to grind riblets with a width of 20 μm and a height of 5 μm. In this process the tool wear amounted to 3 μm after a grinding length of 3000 mm.

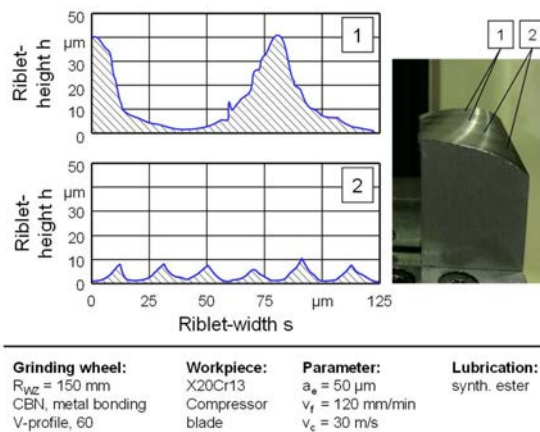
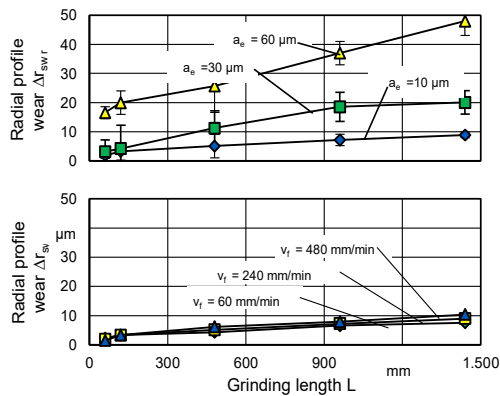


Fig. 7. Riblets on a compressor blade



Nonetheless, it is not clear if this tool can withstand the axial loads and generate ideal riblets on freeform surfaces. To close this gap grinding experiments were done. Due to the resistance to wear, mechanical dressing of metal bonded grinding wheels is difficult. For that reason, electro contact discharge dressing (ECDD) was used to produce the necessary profile geometry. In order to evaluate the wheel profile, the profile height was determined at a profile width of 20  $\mu\text{m}$  and 80  $\mu\text{m}$  respectively. After dressing, the profile height  $h_{20}$  is 7  $\mu\text{m}$  and  $h_{80}$  amounts to 54  $\mu\text{m}$  (fig. 7). Considering the process variation, these profiles are suitable for grinding riblets with a width between 20  $\mu\text{m}$  and 80  $\mu\text{m}$  with an aspect ratio of 0.5. These profiles were used to grind riblets on a compressor blade with a tool path radius of 250 mm. This tool path radius required a maximum grinding wheel radius of 150 mm.

The results of the grinding experiments are shown in fig. 8. The surface of the compressor blade was structured with two different riblet-widths. Riblets had a width of 20  $\mu\text{m}$  and 80  $\mu\text{m}$ . In both cases an aspect ratio of 0.5 could be reached (fig 7). Hence, metal bonded grinding wheels are well suited for grinding riblets on freeform surfaces.



Grinding wheel:	Workpiece:	Parameter:	Lubrication:
$R_{WZ} = 150 \text{ mm}$	X20Cr13	$a_e = 50 \mu\text{m}$	synth. ester
CBN, metal bonding	Compressor blade	$v_f = \text{var.}$	
V-profile, 60		$v_c = \text{var.}$	

Fig. 8. Wear behavior of metal bonded tools

However, industrial application of riblets requires an efficient grinding process. To analyze the efficiency of the grinding process, the influence of feedrate and depth of cut on the tool wear was investigated. Fig. 8 illustrates the tool wear as a function of grinding length for different feedrates and depth of cuts. Independent of feedrate and depth of cut the tool wear increases with the grinding length. However, the influence of the feedrate on the tool wear is small. In contrast, there is a high influence of the depth of cut on the tool wear. This dependency can be explained with thermal loads. In case of mechanical loads the profile wear should depend of the single grain chip thickness. A reduction of the feedrate to 120 mm/min and an increase of the depth of cut leads to a reduction of the single grain chip thickness. If the mechanical loads would affect the tool wear, a reduction of the single grain chip thickness should reduce the tool wear. However, the opposite effect was observed. The depth of cut affects the contact length. A large contact length leads to a difficult

transport of lubricant and chips. Hence, the thermal loads increase caused by many chips and low lubrication within the contact zone. The experiments demonstrate that riblets can be ground on freeform surfaces with a maximum feedrate of 120 mm/min. Due to tool wear, the grinding wheels have to be redressed after a defined grinding length. This length depends on the riblet height and the depth of cut.

The knowledge about the wear behavior was used to design a grinding process for different riblet-dimensions on a compressor blade. The results are shown in fig. 9. The process time is divided into grinding and dressing time. In all cases the amount of dressing time is higher than the grinding time. The total time depends on the riblet sizes and varies between 650 min. for a riblet width of 20  $\mu\text{m}$  and 80 min. for riblets with a width of 60  $\mu\text{m}$ . However, the results verify, that it is possible to grind riblets on a compressor blade, but due to the process time the process is not efficient. Therefore, it is necessary to reduce grinding and overall dressing time.

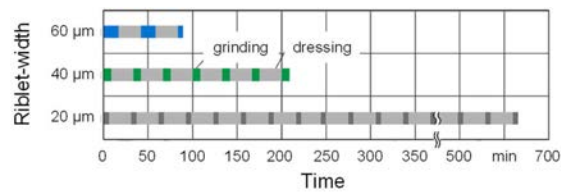


Fig. 9. Efficiency of the grinding process with metal bonded tools

### 3.3. Adjusted grinding wheel

To design an efficient grinding process for structuring of riblets on compressor blades, a new adjusted grinding wheel was developed. This tool is based on the structure of a beaver tooth. The tooth of a beaver has two different layers. In contrast to the inner layer, the outer layer is harder and wears slowly. This different wear behaviour causes a sharp tip of the tooth. This self-sharpening effect is maintained due to continuous growth of the tooth.

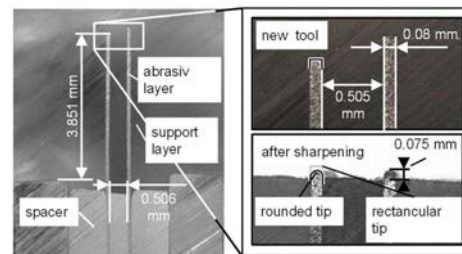


Fig. 10. Prototyp of the new tool design

A grinding wheel build up according to this principle is shown in fig. 10. Here, dicing blades with a width of 80  $\mu\text{m}$  were used for the hard layer. Spacers with a width of 500  $\mu\text{m}$  set a constant distance between these profiles. Finally, synthetic resin was applied as a support layer. Such tools will be dressed with an aluminum oxide stick.

The wear behavior of this new tool can be divided into two different steps. First, the synthetic resin is set back and the abrasive layer tips rounded. The aim of this step is a constant rounding and a protrusion of the abrasive layer. The expected wear behavior was observed in experiments. Grinding wheel cross sections before and after sharpening are presented in

fig. 11. The dicing blade tips are rectangular before and rounded after the sharpening process. The rounding occurs due to higher loads and lower retention force on the edges of the dicing blades.

The second effect during wear protrusion arises in the grinding process. The mechanical and thermal loads set back abrasive as well as support layer. Optimal process parameters lead to a constant wear behavior, which produces a linear decrease of the grinding wheel diameter. Due to this constant set back, additional dressing should not be necessary. Moreover, a constant set back of the grinding wheel can be easily compensated by an adaption of the depth of cut. This strategy is not possible with V-profiles because an increase of depth of cut results in a larger width of the groove. Fig. 11 shows riblets that were ground with the new tools. In all cases the riblets have an aspect ratio of 0.5. The smallest riblets had a width of 25  $\mu\text{m}$  and sharp tips. The sharpness of the tips decreases for larger widths. This can be explained by the tool wear. The slope of the chamfer of the wider tools is not steep enough to create sharp tips. However, grinding wheels with a width of 15  $\mu\text{m}$  requires higher spindle speeds to grind riblets. The tool wear is too high in case of the spindle speed is about 30 m/s. A spindle speed of 80 m/s reduces the wear and riblet structures are formed.

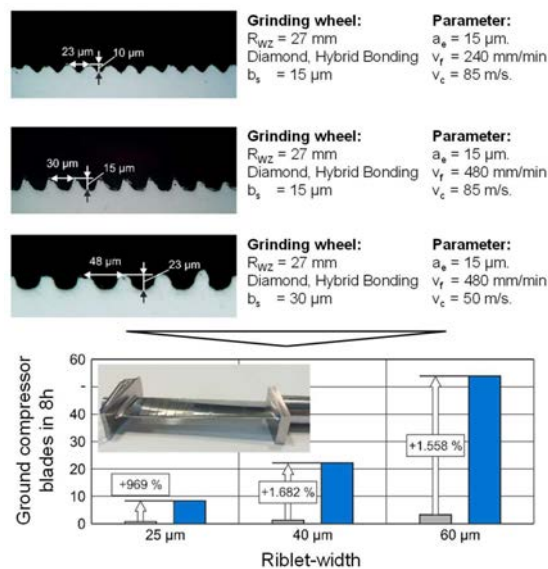


Fig. 11. Ground riblets with the hybrid grinding wheels

Finally, the results were combined to show the benefit of the new tools. Therefore, the dressing and grinding time was calculated for a compressor blade. The new tools do not have to be dressed. It is just necessary to clean them. This cleaning was done after a length of 1000 mm. Compared to the ECDD-process, the time was reduced in average by about 300 min. Additionally, the tools enable higher feedrates. This affects the grinding time. Compared to metal bonded tools the grinding time could be reduced by about 50 min. Overall the number of structured compressor blades per day could be increased by a value between 969 % and 1682 % (fig. 11, bottom)

#### 4. Conclusion

The use of riblets requires an efficient manufacturing process. Grinding with multi-profiled wheels has been established as an effective method for generating riblet-structures on large scale surfaces. The knowledge about grinding of riblets on flat surfaces cannot be transferred to the structuring of real compressor blades. On the one hand, the contact conditions caused undercuts and the riblet-width increase. The results show that undercuts will be avoided when the grinding wheel radius is adapted on the tool path radius. Therefore, a method was introduced in order to calculate the maximum grinding wheel radius. On the other hand, during five axis grinding axial forces occurs and affect high tool wear. As a result, vitrified bonded grinding wheels are not suitable for grinding of riblets on compressor blades. In contrast, metal bonded tools have a better wear behavior and riblets with a width between 20  $\mu\text{m}$  and 80  $\mu\text{m}$  with an aspect ratio of 0.5 were ground. However, this structuring process is not suitable for industrial applications because of the dressing time amount nearly 80% of the whole process time. In order to increase the efficiency, a new grinding wheel design was developed. The new grinding wheel is based on the structure of a beaver tooth and increases the number of structured compressor blades per day by a value between 969 % and 1682 %.

#### Acknowledgements

The investigations described in this paper were undertaken with the support of the Federal Ministry of Education and Research (BMBF) within the VIP-project (03V0473).

#### References

- [1] Malshe A.; Rajurkar K.; Samant A.; Norgaard Hansen H.; Bapat S.; Jiang W.: Bio-inspired functional surfaces for advanced applications, In: CIRP Annals - Manufacturing Technology, Vol 62., pp. 607–628, 2013
- [2] Bechert D.-W.; Bartenwerfer M.: The Viscous Flow on Surfaces with Longitudinal Ribs. Journal of Fluid Mechanics, Vol. 206, pp.105-129, 1989
- [3] Gümmer V.: Pfeilung und V-Stellung zur Beeinflussung der dreidimensionalen Strömung in Leitströmern transsonischer Axialverdichter. Fortschritt-Berichte VDI Reihe 7 Nr. 384, VDI Verlag, Düsseldorf, 2005
- [4] Lietmeyer C.; Hohenstein S.; Naschilevski S.; Seume, J.: Einfluss von Riblet-Strukturen auf den Wirkungsgrad eines Hochgeschwindigkeits-Axialverdichters. Deutscher Luft- und Raumfahrtkongress, 31. August - 02. September 2010
- [5] Pauly C. P.: What is a shark doing in this pump? In World Pumps, pp. 15-16, 2001
- [6] Denkena, B.; Köhler, J.; Wang, B.: Manufacturing of functional riblet structures by profile grinding. In: CIRP Journal of Manufacturing Science and Technology, Vol. 3 (1), pp. 14-26, 2010
- [7] Lietmeyer, C.: Berechnungsmodell zur Widerstandsbeeinflussung nicht-idealer Riblets auf Verdichterschaufeln. Dr.-Ing. Dissertation, Leibniz Universität Hannover, 2012
- [8] Weinert, K.; Blum H.; Jansen, T.; Rademacher, A.: Simulation based optimization of NC-shape grinding process with toroid grinding wheels, In: Production Engineering - Research and Development (WGP), Vol. 1 (3), pp. 245,252, 2007
- [9] Tönshoff, H.K.; Denkena, B.; Böß, V., Urban, B.: Automated Finishing of Dies and Molds, In: Production Engineering - Research and Development 9 (2), pp. 1-4, 2002
- [10] Linke, B.: Wirkmechanismen beim Abrichten keramisch gebundener Schleifscheiben, Dr.-Ing. Dissertation, RWTH Aachen, 2003